

General Disclaimer

One or more of the Following Statements may affect this Document

- This document has been reproduced from the best copy furnished by the organizational source. It is being released in the interest of making available as much information as possible.
- This document may contain data, which exceeds the sheet parameters. It was furnished in this condition by the organizational source and is the best copy available.
- This document may contain tone-on-tone or color graphs, charts and/or pictures, which have been reproduced in black and white.
- This document is paginated as submitted by the original source.
- Portions of this document are not fully legible due to the historical nature of some of the material. However, it is the best reproduction available from the original submission.

TECHNICAL INFORMATION RELEASE

CR-171 876
C.1



management and technical services company

TIR 2114-MED-5006

FROM

Joel I. Leonard, Ph.D.

TO

N. Cintron, Ph.D./SD4

DATE

April 22, 1985

CONTRACT NO:

NAS9-17151

T.O. OR A.D. REF:

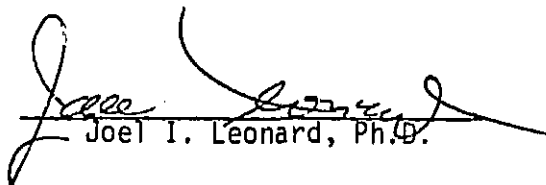
MIS OR OTHER NASA REF:

SUBJECT

Description, Validation, and Modification of the Guyton Model
for Space-Flight Applications

(NASA-CR-171876) DESCRIPTION, VALIDATION, AND MODIFICATION OF THE GUYTON MODEL FOR SPACE-FLIGHT APPLICATIONS. PART A. GUYTON MODEL OF CIRCULATORY, FLUID AND ELECTROLYTE CONTROL. PART E. (Management and Technical G3/52 21223 N85-26122 Unclas 21223

The mathematical model that has been a cornerstone for the systems analysis of space-flight physiological studies is the Guyton model describing circulatory, fluid and electrolyte regulation. This document describes the model and the modifications that were made to permit simulation and analysis of the stress of weightlessness. This material was originally prepared for a NASA Reference Publication.


Joel I. Leonard, Ph.D.

/db

Attachment

Unit

Manager

Approving

Manager

F.A. Kutyna, Ph.D.

NASA

Concurrence

DISTRIBUTION

NASA/HQS:

R. J. White

MATSCO/HQS:

L. Griffiths

NASA/JSC:

BE3/B.J. Jefferson

SA/W. H. Shumate

SB/J. Vanderploeg

SD2/J. Logan

SD3/M. Bungo

/J. Charles

/P. Johnson

/V. Schneider

MATSCO/HO:

R. F. Meyer

Mission Sci.Group

TIR Files

GE/HO:

T.D. Gregory(2)

Contracts File

DESCRIPTION, VALIDATION, AND MODIFICATION OF THE GUYTON MODEL
FOR SPACE-FLIGHT APPLICATIONS

PART A. GUYTON MODEL OF CIRCULATORY, FLUID AND ELECTROLYTE CONTROL

PART B. MODIFICATION OF THE GUYTON MODEL FOR CIRCULATORY, FLUID
AND ELECTROLYTE CONTROL

Prepared by

Joel I. Leonard, Ph.D.

Management and Technical Services Company

Houston, Texas

Prepared for

National Aeronautics and Space Administration

Houston, Texas

Contract NAS9-17151

1985

i.

PART A.

GUYTON MODEL OF CIRCULATORY, FLUID AND ELECTROLYTE CONTROL

Model for Circulatory, Fluid, and Electrolyte Control

Physiologists have long recognized the intimate relationship between circulatory function and fluid-balance function. Early in the manned-space-flight program, the biomedical investigators of NASA identified the need to monitor these systems for their involvement in the fluid redistribution in zero g and the orthostatic intolerance usually accompanying recovery. With the extension of flight duration from weeks to months, the need to examine the long-term adaptive responses of both the circulatory and fluid-balance systems with simulation models was proposed (ref. III-83).

The following objectives were established for a model of body fluid regulation. The desired model should

1. Be capable of predicting the volume and electrolyte composition of the major fluid compartments, including plasma, interstitial, and intracellular fluid compartments
2. Contain the appropriate capillary and membrane interfaces between these compartments and the capability to simulate exchange of fluids and electrolytes under the influence of hydrostatic, oncotic, osmotic, and active transport forces
3. Contain representation of at least two of the major body cations: sodium (extracellular ion) and potassium (intracellular ion)
4. Contain a representation of the kidney with sufficient detail to predict realistic urine excretion of salts and water under such conditions as fluid/salt loading and restricted fluid intake
5. Contain neural, hormonal, and hemodynamic feedback control pathways regulating the volume and composition of the extracellular fluid compartment
6. Contain a circulatory system with sufficient detail to realistically simulate blood pressures, flows, and volumes in arteries and veins during acute and long-term disturbances such as hemorrhage and infusions
7. Contain an autonomic system with efferents sensitive to blood pressure, plasma osmolarity, and tissue oxygenation and with afferents for controlling blood flow and pressures, hormonal secretion (antidiuretic hormone (ADH), angiotensin, and aldosterone), and body water, the latter by thirst and renal mechanisms
8. Contain a representation of adaptation effects (both active and passive) in the heart, vessels, and pressure receptors for controlling long-term blood pressure disturbances

As this list of objectives suggests, the complete specification of a fluid-electrolyte regulatory system requires the inclusion of several fluid compartments which are controlled by the kidneys acting in conjunction with the endocrine and circulatory systems. An important part of the model selection phase of this project was directed toward identifying models that contained these subsystems or, alternatively, searching for fluid-electrolyte models that could be used to complement existing circulatory models (refs. III-84 and

III-85). With regard to the latter approach, most of the mathematical models with the required fidelity to simulate responses to circulatory disturbances were relatively short-term models and did not have the elements necessary to account for changes in fluid balance. On the other hand, the models of fluid-electrolyte regulation had representations of cardiovascular function that were highly simplistic or absent altogether.

The renal system is perhaps one of the most complex body systems amenable to a mathematical modeling approach. When the model identification search was initiated, few models were available that contained an adequate representation of the fluid-electrolyte regulating capability of the renal system. Some of the most detailed models of the kidney were presented as complex mathematical formulations unaccompanied by numerical solutions and they, therefore, remained conceptual in nature (refs. III-86 to III-88). The model of DeHaven and Shapiro (refs. III-89 and III-90) contained excellent representations of the relationships between more than 100 chemical species in several fluid compartments but was devoid of dynamic regulation as well as direct representations of the circulatory, neural, and endocrine systems. Other models considered a number of important conceptual ideas but had characteristics that limited their applicability (refs. III-91 and III-92). Other models of fluid and electrolyte balance include those of Cameron (ref. III-93), Toates and Oatley (ref. III-94), and Badke (ref. III-95); these were unavailable for consideration in this project and are mentioned here merely for completeness.

The most comprehensive model of fluid and electrolyte control available, and one which satisfied the requirements of the project, was that developed by Guyton and co-workers (refs. III-8 and III-96 to III-98). This model has been particularly useful in the NASA physiological simulation project, and it formed the cornerstone of the whole-body algorithm. At the time of its formulation, it was perhaps the most complex physiological mathematical model in existence. There have since been few such comprehensive attempts to subject long-term, whole-body biochemical and circulatory function to the rigors of systems analysis and mathematical modeling which are not directly related to the fundamental work of Guyton.

Description of the Guyton model—The systems analysis of overall circulatory regulation as

developed by Guyton involves a large number of the physiological subsystems. The current model, illustrated in figure III-32, is based on cumulative knowledge of the circulation and on experimental data. A model as complex and encompassing as this one is difficult to summarize in one or two diagrams; detailed flow charts and model explanations are available (refs. III-8, III-84, III-98, and III-99). Schematic diagrams are included in the following pages, and a more detailed analog circuit diagram is included in appendix C.

The relevant physiological systems have been divided into 18 major subsystems, each describing some important physiological aspect of circulatory, fluid, and electrolyte control (fig. III-33). The circuit of blood flow in the original model is divided into five volume compartments: arterial volume, venous volume, right atrial volume, pulmonary venous volume, and combined left atrial and pulmonary venous volume (fig. III-34). Cardiac output is calculated from function curves, whereas other flow rates are calculated from simple pressure-resistance relationships. Arterial-venous flow is determined by summing flow through three parallel circuits (muscle, renal, and other).

The circulation is not closed but "leaks" through the capillaries, "excretes" through the kidneys, and "drinks" directly into the blood. Fluid intake is controlled by plasma osmolarity and tissue oxygen tension. Fluid excretion is based on glomerular filtration and the action of ADH. The blood, composed of plasma (with dissolved proteins and electrolytes) and red blood cells, serves as a filterable fluid. Other fluid-volume compartments include the interstitial compartment (composed of a gel volume and free fluid volume), the intracellular volume, and pulmonary fluid volume. The relationships between these compartments are illustrated in figure III-35. The capillary filtration rate is determined from a whole-body version of Starling's relationship, which states that net filtration pressure is equal to capillary pressure plus tissue colloid osmotic pressure, minus interstitial fluid pressure, and minus plasma colloid osmotic pressure. Lymph flow rate is calculated from free interstitial fluid pressure, total tissue pressure, and lymphatic pumping. Flow into the pulmonary reservoir is obtained by subtracting pulmonary lymph return from pulmonary capillary filtration. Protein (colloid) is produced and lost by the body and is distributed between the interstitial space and the

OF POOR QUALITY

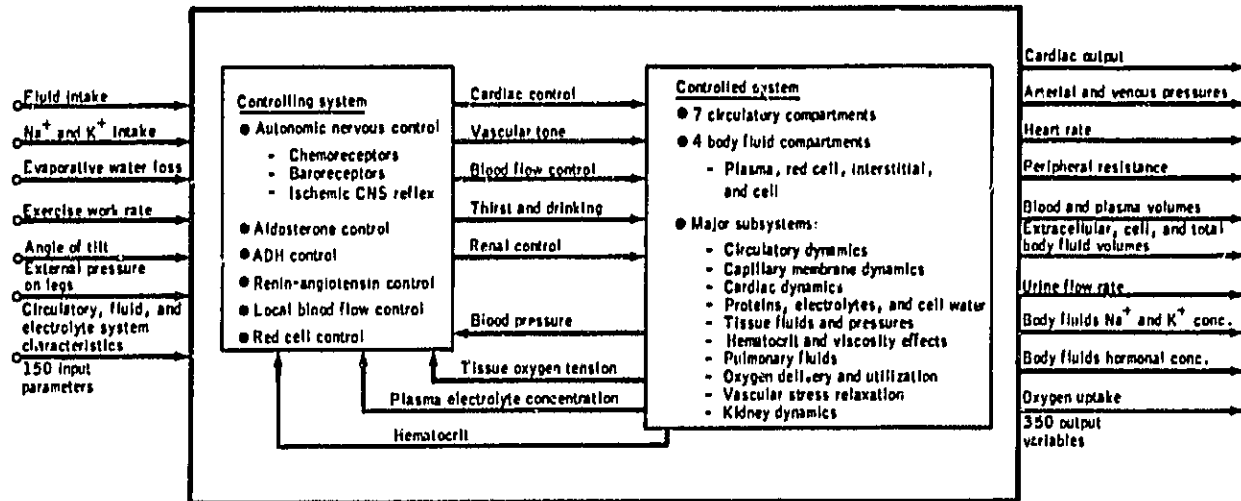


FIGURE III-32.—Schematic diagram of the circulatory, fluid, and electrolyte regulatory model.

plasma. The representation of the interstitial fluid compartment reflects the years of study by Guyton and co-workers which revealed the importance of the gel-free fluid matrix and subatmospheric pressures of this compartment in controlling edema and transcapillary filtration. Fluid flows into the cells are assumed to occur by osmotic imbalance between extracellular and intracellular fluids.

Two electrolytes are considered in the model. Sodium is distributed evenly in the extracellular fluid, and potassium is stored primarily in the intracellular fluid with allowance for active transport from the extracellular to the intracellular compartments. Dietary intake of both these electrolytes is considered as well as renal excretion, the latter being controlled in large part by a renin-angiotensin-aldosterone mechanism. The pathways that regulate fluid and electrolyte balance are described in more detail in Section V.

The model uses basic cardiac function curves modified by the effects of autonomic stimulation, arterial pressure afterload, and cardiac hypertrophy or degeneration of the pumping ability of the heart. The unstressed volumes of each capacitive region are controlled by the level of autonomic stimulation, the level of angiotensin in the blood, and the pressure in the veins (through stress relaxation). The flow resistances are controlled by a combination of local effects and hormonal effects. The oxygen transport features of the circulation are present, and hematocrit and red cell control are considered. The autonomic system included is

basically regulated by mean blood pressure and tissue oxygen tension and includes the effects of the baroreceptors, chemoreceptors, and ischemia of the central nervous system. Total autonomic output is expressed as a positive effect for sympathetic output and a negative effect for parasympathetic output.

Comparison of the blood flow circuit in the Guyton model (fig. III-34) to that of the Croston model shows a great difference in the number of volume segments. These differences reflect a higher fidelity response for short-term stresses in the latter model. However, the Croston model as well as the other models described earlier have used a basic closed circulatory flow system with no leaks. This kind of approach can be justified when the simulated challenge is acute. When longer duration simulations are required, a large number of other regulatory mechanisms must be included to describe overall circulatory control, even in a crude manner. The lack of detail in Guyton's circulatory subsystem can be contrasted with the complexity of the connections between the cardiovascular system and the interstitial-cell complex. The inclusion of such elements as cardiac hypertrophy, cardiac deterioration, baroreceptor adaptation, hormonal pathways, regeneration of red blood cells and plasma proteins, delayed autoregulation of resistance vessels, and stress relaxation of veins clearly indicates that the Guyton model was developed to be useful as a long-term model. This feature has made it very attractive as a companion

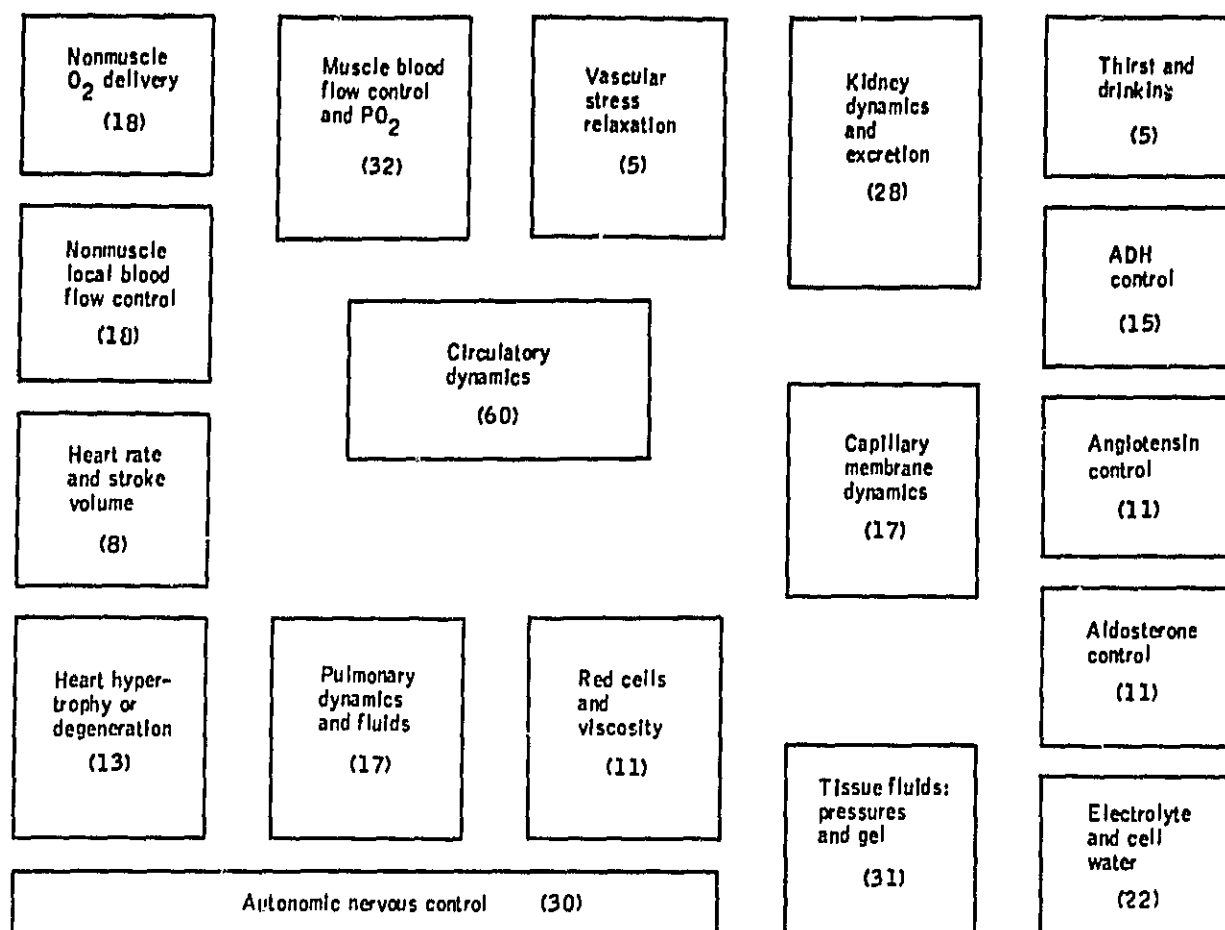


FIGURE III-33.—Composition of Guyton model of the circulatory, fluid, and electrolyte system. Each block represents a subsystem which consists of a family of function blocks indicated by the numerical figure in parentheses. Modified from reference III-4.

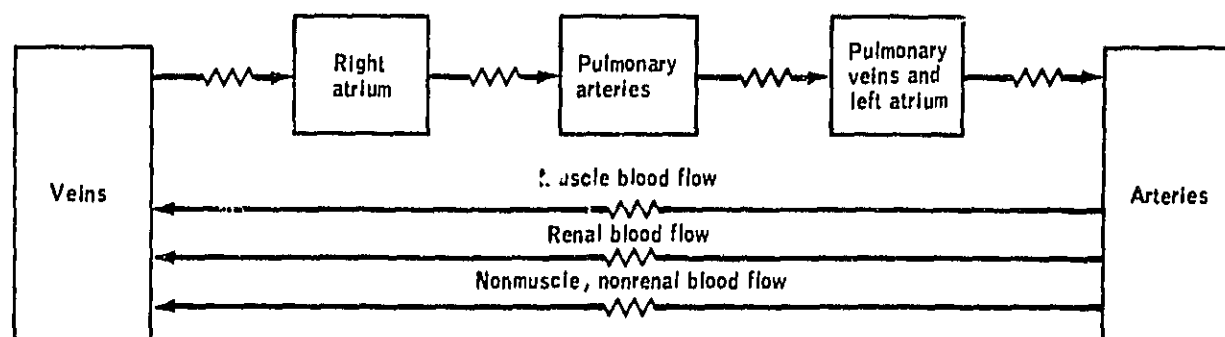


FIGURE III-34.—Blood volumes and flows in the original Guyton model.

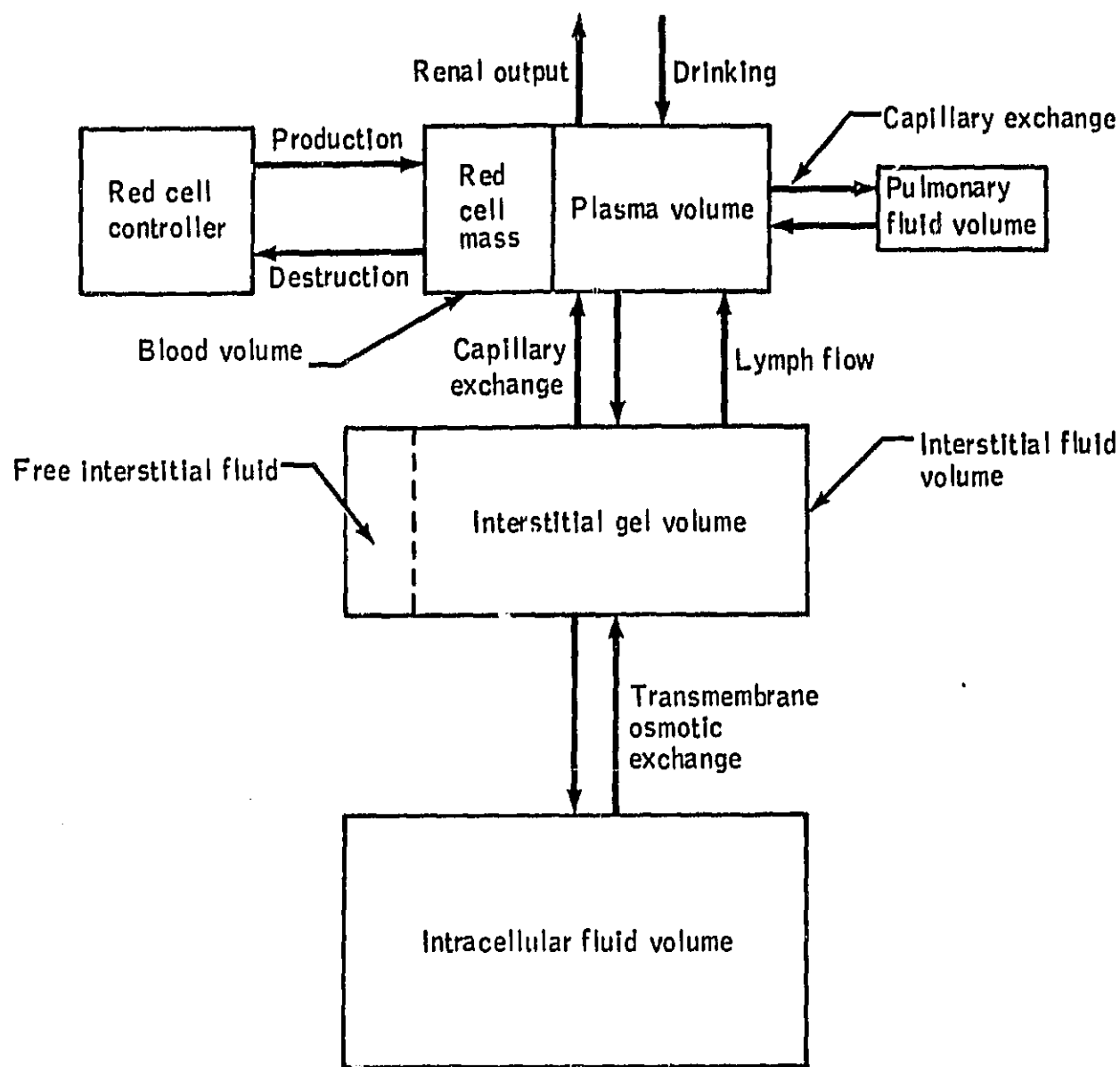


FIGURE III-35.—Fluid-containing reservoirs of original Guyton model. The volume of each compartment is controlled by active and passive regulators.

to a short-term pulsatile model for the whole-body algorithm application.

The evolution of the Guyton model from a basic circulatory system to a much more complex grouping of subsystems revealed that a model of the cardiovascular system must include elements from most of the entire body if it is to be used in the study of intermediate to long-term phenomena. The Guyton model clearly illustrates the importance of considering the interaction between

various subsystems in predicting fluid volumes and electrolyte levels. The real system and the model itself are extremely stable, so much so, in fact, that the function of any single control mechanism can be in error by as much as 50 percent without significantly affecting the overall output of the system. One of the most important features of this model is that it is large enough to obtain this stability level, similar to that in the real system, despite the fact that each subsystem is modeled in a gross sense

with many minute details omitted. Because of this stability, the model is adequate for predicting the outcome of many long-term experiments.

The system of equations representing this closed-loop model contains more than 370 mathematical relationships and is a large, stiff system with response times ranging from 0.5 second to 40 days. Numerical integration over extended periods would be extremely time consuming unless special techniques were employed. The basic method of integration is a variant of the simple Euler method made possible by the fact that, for many simulations, all short-term subsystems can be separated from the rest of the model and integrated many times using small time steps without disturbing the remainder of the system. When these rapidly acting subsystems have developed near steady-state values, the remainder of the system is numerically integrated, using a relatively large time step, and the whole process is repeated. This procedure is only possible when slow, nonvascular changes are taking place. With rapid overall transitions, as in exercise, a small integration step must often be used for the entire system, greatly slowing the model simulation.

Guyton model limitations and modifications—The original Guyton model was built to simulate a large number of diverse situations, but there were some specific stresses for which the model response was inadequate. Since the model did not include separate vascular compartments representing the legs, the model was incapable of responding to either gravitational or postural changes. Analysis of Skylab data has shown that the rapid shifts of fluid from the lower to the upper body as well as a more gradual dehydration of leg tissues play a very important role in the physiological adaptation to zero g (refs. III-100 and III-101). The data from bed-rest studies, taken as a ground-based experimental analog to zero g, have also shown similar important changes involving the legs (ref. III-102).

There have been a few studies in which the gravitational effects of posture on the body fluid compartments have been modeled. However, no studies have been done to account for long-term simulation of gravity disturbances such as bed rest or weightlessness. Models of the circulatory system that contain short-term gravity effects have met with various degrees of success. The models of short-term circulatory gravity effects include those of Snyder (ref. III-15), Croston et al. (ref. III-10), and Green and Miller (ref. III-103). Several studies

by Luetscher and co-workers (refs. III-104 to III-106) resulted in models that included the effects of intravascular-interstitial fluid shifts on circulatory and renal responses to postural change and, thereby, allowed for slightly longer term simulations. These latter models, however, were not designed to account for even longer term effects such as lymph return, extravascular protein circulation, and hormonal effects. Nevertheless, the ideas embedded in these models were useful in altering the Guyton model.

The circulatory subsystem of the Guyton model contained only two lumped systemic blood compartments representing the arteries and veins. Modifications made to the model included increasing the number of compartments of the circulatory system so that lower body (i.e., legs) and upper body blood and tissue fluid compartments could be identified separately and adding gravity effects on blood flow and baroreceptor elements to permit the new circulatory system to respond to a variable gravity vector. These modifications are illustrated in figure III-36.

Cardiac output was divided into three pathways, as previously described. However, flow through the legs was taken to be the same as the muscle flow of the original model. In addition, a filterable capillary bed was added to this pathway. Details of these modifications are discussed in appendix C. These changes added the basic capabilities to simulate such stresses as postural change (tilt, including head-up and head-down), LBNP, bed rest, and weightlessness.

Other modifications to the Guyton model, introduced during the course of this project, included alterations in the renin-angiotensin system, the baroreceptor system, the stress relaxation of the vasculature, the autoregulation of muscle blood flow, and the red blood cell control system. Most of these changes were not made because of limitations of the model for space-flight applications; they were made because other ground-based physiological studies revealed that their inclusion would be more appropriate. Details of these modifications, including the changes for gravity dependency, are available in two study reports (refs. III-99 and III-107) as well as in appendix C.

One weakness in the Guyton model, for some special circumstances, is the lack of a description of hydrogen-ion regulation (i.e., acid-base balance). Hydrogen-ion levels are controlled by the renal system, the buffering system of the body, and the

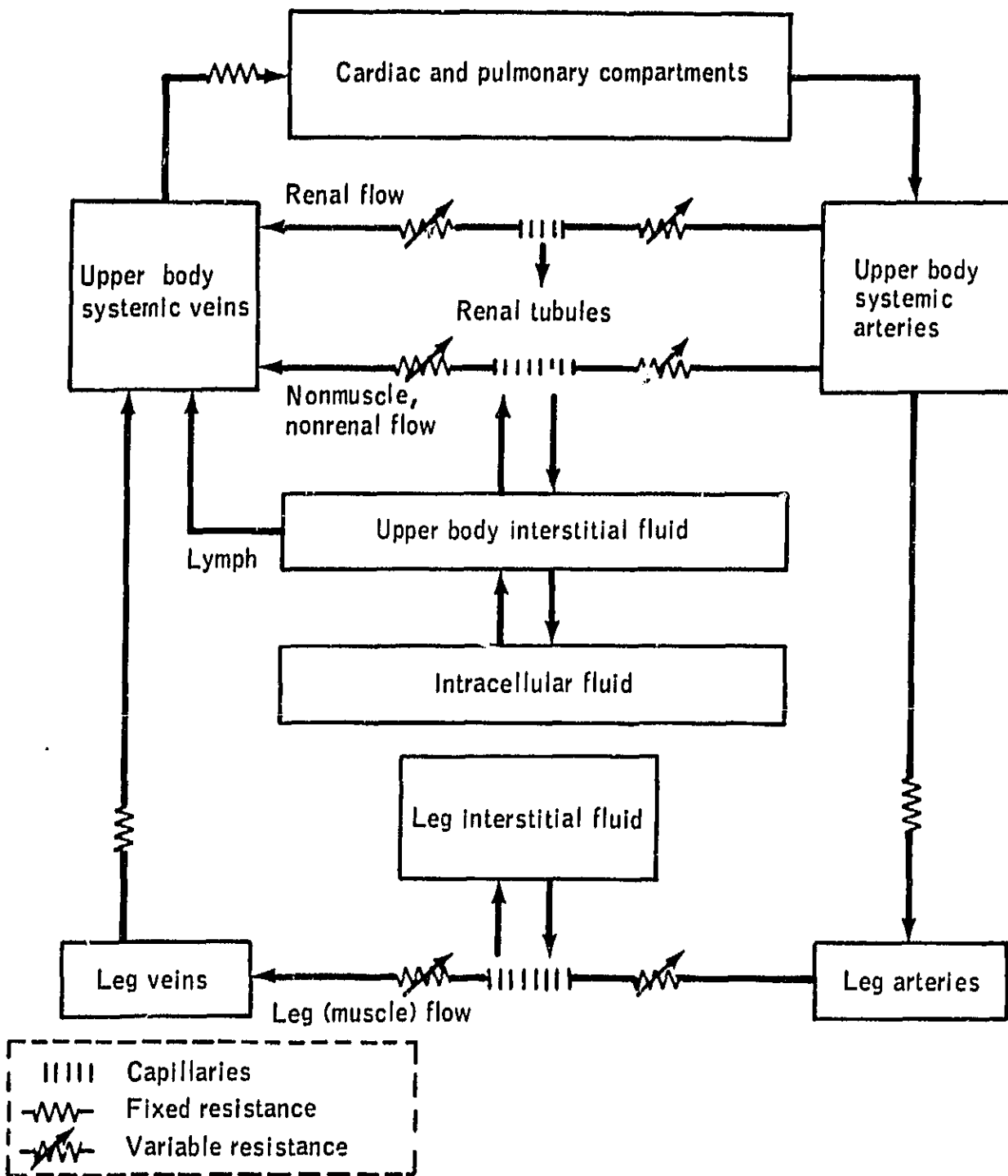


FIGURE III-36.—Circulatory and fluid compartments in modified Guyton model. Leg blood and interstitial compartments have been added. Gravity influences carotid baroreceptors and blood flow in legs.

respiratory system, all acting together. In fact, the hydrogen-ion control system is one of the main links between the circulatory, renal, and respiratory systems. A preliminary analysis which lays the foundation for a model of this valuable subsystem was performed during this project (ref. III-99), and other researchers have studied this subsystem in some detail (ref. III-108).

In the latter stages of this project, it has become apparent that new techniques are required to simulate the weightlessness of space flight and its ground-based experimental analogs such as water immersion and head-down bed rest. These stresses were never contemplated in the design of the original Guyton model. Some of the required features which have been identified include collapsible leg veins, fluid reservoirs above the heart (i.e., jugular vein system and head tissues), and orthostatic mechanisms. The latter elements would allow the model to assume an upright reference position in addition to its present supine reference. These modifications are discussed in Section VI.

Validation of the basic Guyton model.—The formulation of the Guyton model was based on a wide variety of experimental data, and the model has been tested extensively. Some of the experiments that have been performed with this model are simulation of the development of hypertension in a salt-loaded, renal deficient patient and simulation of congestive heart failure, nephrosis, circulatory changes during severe muscle exercise, and unilateral heart failure of the right or left side. Other simulations performed were of the effects of the removal of the sympathetic nervous system on circulatory function, infusions of various types, and the effects of extreme reduction of renal function on circulatory function. The model performed adequately in almost every case. These initial validation studies are discussed in reports issued by Guyton and co-workers (refs. III-8, III-96, III-98, and III-109).

The capability of the Guyton model to predict the appropriate response to fluid-volume shifts in the space-flight environment was established more easily and convincingly by suitable validation studies based on ground-based experiments. (See table III-2.) The basic model itself was based on detailed organ level studies and required almost 20 years to develop. However, Guyton and his co-workers were more interested in developing a model for hypertension research and did not report model responses for the stresses directly relevant

to space flight. Since the weightless state is associated with initial expansion of the central blood volume and subsequent partial depletion of plasma and body fluids, the model was validated for such common one-g stresses as infusions and dehydration for which much data are available.

Several of these studies are illustrated in figures III-37 to III-39. The first two figures illustrate the responses to fluid-electrolyte infusions and the third demonstrates the response to dehydration and subsequent rehydration. In all cases, a variety of infusions was performed, including those of hypertonic, isotonic, and hypotonic fluid. The model is capable of distinguishing between variations in the tonicity of the infusion.

In the first series of simulations (fig. III-37), 1 liter of water, 150 milliequivalents sodium, and 1 liter of isotonic saline (1 liter water plus 150 milliequivalents sodium), respectively, were infused. These infusions were made directly into the circulation, so that the response was more rapid and more dramatic than if they had been administered orally. The three infusions all produce appropriate osmotic shifts between extracellular/intracellular spaces and renal excretions of salt and water, as well as proper hormonal responses. Similar responses would be expected for the human subject (refs. III-112 and III-113). For water infusion, the diuresis is completed within the first few hours. For isotonic saline, the diuresis is maintained at a lower level but continues beyond several hours. In the case of water or sodium infusion, large variations in cell fluid volume are observed, whereas in the case of isotonic saline, the cell fluid volume is essentially unaffected. Antidiuretic hormone was also appropriately responding to osmotic concentrations of extracellular fluid (ref. III-114), decreasing rapidly in the case of the water infusion, increasing threefold in the case of pure sodium, and barely changing in the case of isotonic saline. Aldosterone in the model is regulated by angiotensin, extracellular potassium, and extracellular sodium. It reacted appropriately to the primary stress of these experiments by showing a change in extracellular sodium concentration in the first two cases and a fall in angiotensin (not shown) in the last case, due to increased renal arterial pressure. Experiments such as these illustrate the importance of electrolyte considerations in water-balance studies, a concept quite familiar to most clinicians.

A more detailed study of an isotonic saline infusion, particularly as it affects plasma-interstitial

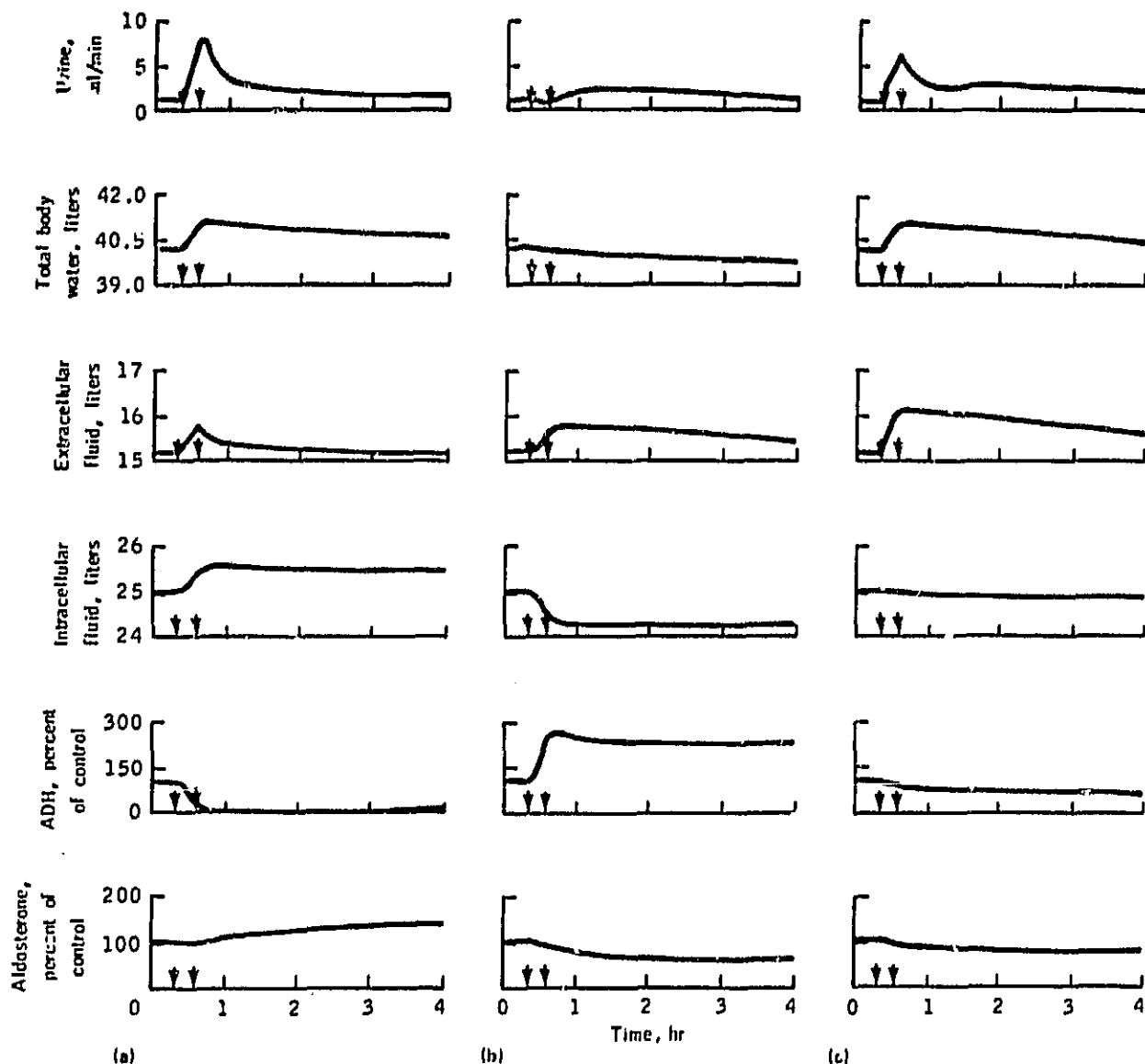


FIGURE III-37.—Simulated infusion responses using circulatory, fluid, and electrolyte model. These studies demonstrate capability of model to distinguish between the tonicity of fluids in acute water and salt loading. Arrows demarcate infusion period. (a) Infusion: 1000 milliliters water (hypertonic). (b) Infusion: 150 milliequivalents sodium (hypertonic). (c) Infusion: 1000 milliliters saline (isotonic).

fluid exchange, is shown in figure III-38. The simulation consisted of a 2-liter transfusion over a 30-minute period into a nephrectomized subject. Capillary filtration increases markedly as the transfusion begins and lymph return increases more slowly, resulting in a net outward flow of fluid from the plasma. Since net flow into the interstitial space is less than the transfusion rate, fluid accumulates in the plasma, and plasma

volume increases considerably. When the transfusion is stopped, capillary filtration falls to equal lymph flow, and the interstitial fluid continues to expand at the expense of plasma volume until transcapillary flow is reduced and equals lymph flow. At the end of the transfusion, 37 percent of the added fluid remained in the plasma, but within 30 minutes, only 24 percent of the transfusion volume remained. If the transfusion had been large

enough, the interstitial fluid compartment would have entered the region of low compliance and almost all additional fluid beyond a certain point would have entered the interstitial space. The results of this simulation compare quite favorably with recent experiments (ref. III-115) and demonstrate the suitability of this model for studying

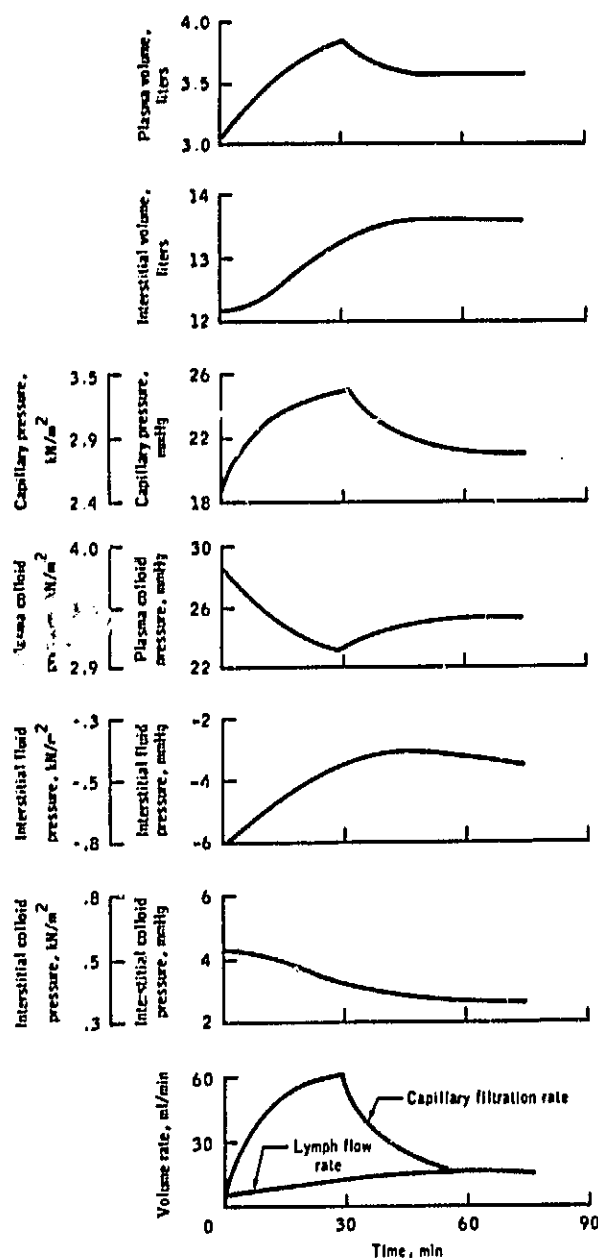


FIGURE III-38.—Simulation of isotonic saline infusion showing capillary filtration responses in nephrectomized subject (from ref. III-110).

situations involving fluid shifts and circulatory function.

Model validation was also extended to include such similar stresses as hemorrhage, salt depletion, and salt loading—for both short-term and long-term changes. Rehydration through use of various fluids has different effects on plasma-volume recovery. In these studies, shown in figure III-39, and others not shown, interstitial fluid does not always act like the fluid reservoir that some investigators have claimed (ref. III-116). Following simulated hemorrhage, for example, the interstitial space provides only 20 percent of the acute plasma refilling response. This has also been noted experimentally by others (ref. III-117). After dehydration

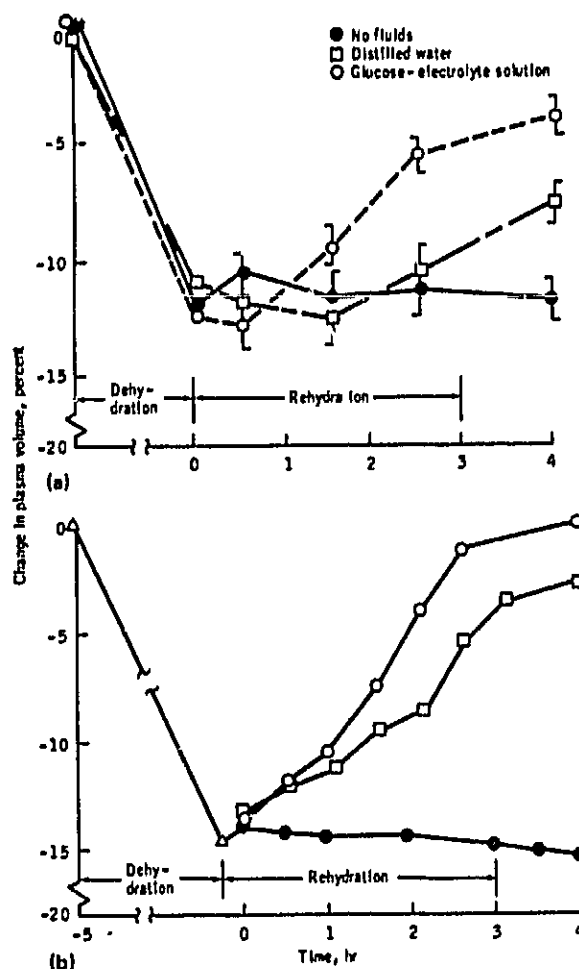


FIGURE III-39.—Plasma volume response to thermal dehydration and subsequent rehydration with fluids of different tonicity: Guyton model response compared to data. (a) Experimental data (ref. III-111). (b) Computer simulation.

without rehydration, there is very little tendency for acute refilling of blood either in the model or in the real system. Also, after infusion, the interstitial compartment first expands but, within 24 hours, returns to normal. This has relevancy to the Skylab experience, in which inflight losses from all fluid compartments were observed to change except for the interstitial space.

Simulations that are even more relevant to the zero-g model validation are the water-immersion studies discussed in Section VI. Where appropriate, the model was modified slightly in accordance with more recent experimental evidence.

Validation of leg compartments and gravity functions—Although the validation studies cited are related to the fluid shifts associated with weightlessness, they do not directly evaluate the capabilities of the model concerned with leg recompartmentation and gravity dependency. The modified Guyton model was validated for the following four conditions. (Results of these studies are presented in other portions of this publication.)

1. *Supine mode at rest*—The Guyton model is initialized in a so-called "supine position." That is, the values of such quantities as heart rate, blood pressure, and cardiac output agree with measurements from human subjects in the resting horizontal (supine) position. Steady-state values for the gravity-dependent model in the supine, unstressed mode should have agreed with those of the original unmodified model, and they did. This test does not really represent a validation study; however, it was important to ensure that the modifications did not change the basic output variables of the model such as cardiac output, mean arterial pressure, fluid volumes, concentrations, and renal function. In addition, for the sake of consistency, values of flows, pressures, and volumes of the new lower body compartment should compare favorably with the pulsatile cardiovascular model (Croston model) and with available data on human subjects who are supine for relatively short periods. Documentation of this study is given in reference III-107.

2. *Supine mode under stress*—The restructured model responded to various supine stresses in a manner essentially similar to that of the original model. The stresses were those already discussed in the section describing the validation of the basic Guyton model. In addition, the capability to perform LBNP simulations was demonstrated. Simulation results for this stress were compared with results of the pulsatile cardiovascular model

that were previously validated for LBNP. The Guyton model did not exhibit the same degree of accuracy as the Croston model for some cardiovascular indices during LBNP; however, the capability to account for capillary fluid shifts was more realistic (ref. III-107).

3. *Standing mode at rest*—Quiet standing results in different values of circulatory parameters (i.e., cardiac output, blood pressures, hematocrit) than those found in the supine position. Changing posture from supine to upright represents a stress to the individual and a suitable challenge to the model. Values of basic circulatory parameters in the standing mode should agree with data from human subjects performing quiet standing or tilt for relatively short periods of time. The model contains the capability to vary the angle of tilt with respect to gravity but does not include protective orthostatic mechanisms. These simulations of passive tilting and erect standing suggested new elements in the model to account for muscle pumps, venous valves, abdominal compression reflex, and venoconstriction, all of which are important in the real system to prevent orthostatic collapse (ref. III-107). The additional lower body compartment realistically simulated blood pooling, extravascular filtration, and peripheral vasoconstriction. Comparison of responses was made not only with human data but also with simulation responses from the models of other investigators. The "open" nature of Guyton's circulatory system was expected to provide increased fidelity for simulations of tilt and LBNP. Extremely long-term effects of standing at rest without leg activity will result in continued pooling of blood in the legs, but these effects were not considered. The capability to simulate long-term stress was demonstrated only in the supine position.

4. *Long-term bed rest*—Long-term bed rest can be considered a special case of the supine mode. However, the Guyton model (already initialized in the supine position) required additional modification and hypotheses to simulate the headward shifts of fluids and the dehydration of leg tissues; both are characteristics of bed rest. Incorporation of the lower body segments into the Guyton model and the successful completion of the studies outlined previously has provided a solid foundation and the necessary level of detail with which to test theories of long-term adaptation, including weightlessness. The validation studies discussed

here (LBNP, postural change, and long-term bed rest) are described in Section VI.

The Guyton model represents an attempt to understand the interactions between acute and long-term adaptive control of the body fluids and the circulation. Because there is a notable scarcity of information regarding these complex processes in healthy subjects, long-term bed rest and space flight have been of particular importance in validating and modifying the original model of Guyton. This model is clearly relevant to space flight because some of the most notable physiological changes that occur can be traced to disturbances in fluid-electrolyte regulation. By accounting for long-term adaptive effects in the circulatory and autonomic systems, the model has been useful in predicting responses to stresses lasting up to several weeks or months.

REFERENCES

- III-10 Croston, R. C.; Rummel, J. A.; and Kay, F. J.: Computer Model of Cardiovascular Control System Responses to Exercise. *Trans. ASME Ser. G: J. Dyn. Sys. Meas. & Cont.*, vol. 95, no. 3, Sept. 1973, pp. 301-307.
- III-15 Snyder, Maurice Francis: A Study of the Human Venous System Using Hybrid Computer Modeling. Ph.D. Dissertation, University of Wisconsin, 1969.
- III-83. Physiology in the Space Environment. Vol. I, Circulation. Publication 1485 A, National Academy of Sciences, National Research Council (Washington, D.C.), 1968.
- III-84. White, R. J.: Summary Report on a Basic Model of Circulatory, Fluid, and Electrolyte Regulation in the Human System Based Upon the Model of Guyton. (General Electric Co., Houston, Tex.; TIR 741-MED-3042.) NASA CR 160121, 1973.
- III-85. Kuchar, N. R.; and Sittel, K.: Modeling and Integration of Physiological Control Systems. Final Report, Contract NAS 9-11657. (General Electric Co., Houston, Tex.) NASA CR-160121, 1973.
- III-86. Jacques, John A.; Carnahan, Brice; and Abbrecht, Peter: A Model of the Renal Cortex and Medulla. *Math. Biosci.*, vol. 1, no. 2, 1967, pp. 227-261.
- III-87. Alvi, Z. M.; and Lyman, J. H.: Development of a Mathematical Model for the Nonequilibrium Kinetics of Major Electrolytes in the Human Body. Tech. Rep. no. 45, Biotechnology Laboratory, University of California at Los Angeles, June 1969.
- III-88. Levine, Sumner N.: A Model for Renal-Electrolyte Regulation. *J. Theor. Biol.*, vol. 11, no. 2, July 1966, pp. 242-256.
- III-89. DeHaven, J. C., and Shapiro, N. Z.: Intrinsic Control of Body Fluid and Electrolyte Distribution and Urine Formation. Rep. RM-4609-PR, The Rand Corp. (Santa Monica, Calif.), 1965.
- III-90. DeHaven, J. C.; and Shapiro, N. Z.: Simulation of the Renal Effects of Antidiuretic Hormone (ADH) in Man. *J. Theor. Biol.*, vol. 28, no. 2, Aug. 1970, pp. 261-286.
- III-91. Koshikawa, S.; and Suzuki, K.: Study of Osmo-Regulation as a Feedback System. *Med. & Biol. Eng.*, vol. 6, no. 2, Mar. 1968, pp. 149-158.
- III-92. Reeve, Ernest Basil; and Kulhanek, Leslie James: Regulation of Body Water Content: A Preliminary Analysis. *Physical Bases of Circulatory Transport: Regulation and Exchange*, E. B. Reeve and A. C. Guyton, eds., W. B. Saunders Co. (Philadelphia), 1967, pp. 151-177.
- III-93. Cameron, W. Hugh: A Model Framework for Computer Simulation of Overall Renal Function. *J. Theor. Biol.*, vol. 66, no. 3, 1977, pp. 551-572.
- III-94. Toates, F. M.; and Oatley, K.: Computer Simulation of Thirst and Water Balance. *Med. & Biol. Eng.*, vol. 8, no. 1, Jan. 1970, pp. 71-87.
- III-95. Badke, F.: Further Development of a Model of Human Salt and Water Regulation. *Trans. ASME Ser. G: J. Dyn. Sys. Meas. & Cont.*, vol. 95, no. 3, Sept. 1973, pp. 259-264.
- III-96. Guyton, Arthur C.; and Coleman, Thomas G.: Quantitative Analysis of the Pathophysiology of Hypertension. *Circulation Res.*, vol. XXIV, Suppl. 1, Hypertension—vol. XVII, Experimental Hypertension, May 1969, pp. 1-1-1-20.
- III-97. Guyton, A. C.; Coleman, T. G.; et al.: Systems Analysis of Arterial Pressure Regulation and Hypertension. *Ann. Biomed. Eng.*, vol. 1, Dec. 1973, pp. 254-281.
- III-98. Guyton, A. C.; Coleman, T. G.; et al.: Relationship of Fluid and Electrolytes to Arterial Pressure Control and Hypertension: Quantitative Analysis of an Infinite-Gain Feedback System. *Hypertension: Mechanisms and Management*, G. Onesti, K. E. Kim, and J. H. Moyer, eds., Grune and Stratton (New York), 1973.
- III-99. White, R. J.: A Long Term Model of Circulation. Final Report. (General Electric Co., Houston, Tex.; TIR 741-MED-4021.) NASA CR-147674, 1974.
- III-100. Hoerner, G. W.: Cardiovascular Studies of U.S. Space Crews: An Overview and Perspective. *Cardiovascular Flow Dynamics and Measurements*, N. H. C. Hwang and N. A. Normann, eds., University Park Press (Baltimore), 1977, pp. 335-363.

- III-101. Thornton, William E.; and Hoffer, G. Wyckliffe: Hemodynamic Studies of the Legs Under Weightlessness. Biomedical Results From Skylab. Richard S. Johnston and Lawrence F. Dietlein, eds., Sec. V, Cardiovascular and Metabolic Function, ch. 31. NASA SP-377, 1977, pp. 324-329.
- III-102. Greenleaf, John E.; Greenleaf, Carol J.; VanDerVeer, Dena, and Dorchak, Karen J.: Adaptation to Prolonged Bedrest in Man: A Compendium of Research. NASA TM X-3307, 1976.
- III-103. Green, J. F.; and Miller, N. C.: A Model Describing the Response of the Circulatory System to Acceleration Stress. *Ann. Biomed. Eng.*, vol. 1, Dec. 1973, pp. 455-467.
- III-104. Boyers, D. G.; Cuthbertson, J. G.; and Luetscher, J. A.: Simulation of the Human Cardiovascular System: A Model With Normal Responses to Change of Posture, Blood Loss, Transfusion, and Autonomic Blockade. *Simulation*, vol. 18, June 1972, pp. 197-206.
- III-105. Luetscher, John A.; Boyers, David G.; Cuthbertson, James G.; and McMahon, David F.: A Model of the Human Circulation: Regulation by Autonomic Nervous System and Renin-Angiotensin System, and Influence of Blood Volume on Cardiac Output and Blood Pressure. *Circulation Res.*, vol. XXXII, Suppl. 1, Hypertension—vol. XXI Hypertension in Man and the Experimental Animal, May 1973, pp. 1-84-1-98.
- III-106. Luetscher, J. A.; Boyers, D.; and Resneck, J.: Control of the Renal Circulation and Kidney Functions. *Proceedings of the Summer Computer Simulation Conference (San Diego, Calif.)*, 1972, pp. 1099-1109.
- III-107. Leonard, J. I.; and Grounds, D. J.: Study Report: Modification of the Long Term Circulatory Model for the Simulation of Bed Rest. (General Electric Co., Houston, Tex.: TIR 742-LSP-7011.) NASA CR-160186, 1977.
- III-108. Ikeda, N.; Marumo, F.; Shirataka, M.; and Sato, T.: A Model of Overall Regulation of Body Fluids. *Ann. Biomed. Eng.*, vol. 7, 1979, pp. 155-166.
- III-109. Guyton, Arthur C.; Granger, Harris J.; and Taylor, Aubrey E.: Interstitial Fluid Pressure. *Physiol. Rev.*, vol. 51, no. 3, July 1971, pp. 527-563.
- III-112. Guyton, A. C.: *Textbook of Medical Physiology*. Fifth ed. W. B. Saunders Co. (Philadelphia), 1976.
- III-113. Bland, John H.: General Clinical Considerations in Water, Electrolyte and Hydrogen Ion Metabolism. *Clinical Metabolism of Body Water and Electrolytes*, ch. 8. W. B. Saunders Co. (Philadelphia), 1963, pp. 165-224.
- III-114. Dunn, Fredrick L.; Brennan, Thomas J.; Nelson, Aerial E.; and Robertson, Gary L.: The Role of Blood Osmolality and Volume in Regulating Vasopressin Secretion in the Rat. *J. Clin. Invest.*, vol. 52, no. 12, Dec. 1973, pp. 3212-3219.
- III-115. Leonard, Joel I.; and Abbrecht, Peter H.: Dynamics of Plasma-Interstitial Fluid Distribution Following Intravenous Infusions in Dogs—An Experimental and Computer Simulation Study. *Circulation Res.*, vol. XXXIII, no. 6, Dec. 1973, pp. 735-748.
- III-116. Gauer, O. H.; Henry, J. P.; and Behn, C.: The Regulation of Extracellular Fluid Volume. *Ann. Rev. Physiol.*, vol. 32, 1970, pp. 547-595.
- III-117. Gann, Donald S.; and Pirkle, J. Carl: Role of Cortisol in the Restitution of Blood Volume After Hemorrhage. *American J. Surg.*, vol. 130, no. 5, 1975, pp. 565-569.

PART B.

MODIFICATION OF THE GUYTON MODEL FOR CIRCULATORY, FLUID AND
ELECTROLYTE CONTROL

Modifications of the Guyton Model for Circulatory, Fluid, and Electrolyte Control

The original version of the model developed by Arthur Guyton and used extensively as a basis for much of this work was built as a general-purpose model of overall circulatory regulation and was used to simulate a wide variety of real situations, including congestive heart failure, various types of hypertension, fistula, and hypoproteinemia (refs. C-1 and C-2). Despite these successes, the model, as originally constructed, did not have the level of detail required to respond to the challenge of the microgravity environment, and changes were made in the original model to enable studying the responses to this challenge in more detail. These modifications are available in report form (refs. C-3 and C-4), but they are presented and summarized here for the convenience of the interested reader.

The original version of the Guyton model is presented in figure C-1. A legend of symbols, definitions, and units is included. In addition, Fortran language versions of both the original and the modified model are obtainable (refs. C-5 and C-6).

The following discussion summarizes the modifications that were concerned primarily with recompartmenting the circulatory subsystem to include leg volume and controller elements; adding gravity-dependent functions to the controlled and controller systems; and revising and updating the red blood cell block, the angiotensin block, and the baroreceptor block. These modifications have extended the capability of the original model so that the effects of gravity removal on fluid distribution may be simulated more realistically.

LEG CIRCULATORY COMPARTMENT

Two additional compartments have been added to the model of the circulatory system, one to represent the arteries in both legs and the other to represent the veins. (See fig. III-36.) Each compartment is characterized by a total blood volume, blood pressure, and compliance. (See table C-1.) The values for volumes and compliances of the leg compartments were derived from the model of the 28-compartment pulsatile cardiovascular sub-

system of the whole-body algorithm. The blood volumes and compliances of the upper circulatory compartments were adjusted to keep the total volume and compliance of the arterial and venous vessels nearly identical to those in the original Guyton model.

BLOOD FLOW PATHWAYS AND METABOLIC RATES

The original Guyton model contained three blood flow pathways: renal, muscle, and the rest of the circulation. In the modified version, these three pathways remain intact; however, the muscle flow pathway represents the entire leg flow, and the nonmuscle, nonrenal pathway together with the renal flow represents total upper body flow. In this modified model, leg blood flow and muscle blood flow are identical. Muscle and nonmuscle, nonrenal flows were readjusted by changing their basic resistances so that cardiac output was similar to that of the unmodified version of the Guyton model and leg flow was similar to that of the leg blood flow of the short-term pulsatile cardiovascular model of the whole-body algorithm. Metabolic demand in terms of oxygen consumption was also readjusted in proportion to the new blood flow rates.

RESISTANCES OF THE LEG BLOOD VESSELS

The single resistance in the muscle blood flow pathway of the original version was replaced by two variables in series to allow capillary filtration to occur in the muscles. These represent a precapillary arteriolar resistance and a postcapillary venular resistance, the values of each being dependent on autonomic and angiotensin effects. In addition, the venular resistance responds to passive distention due to hydrostatic pressure, whereas the arteriolar resistance includes autoregulatory and viscosity effects. These formulations for the leg muscle

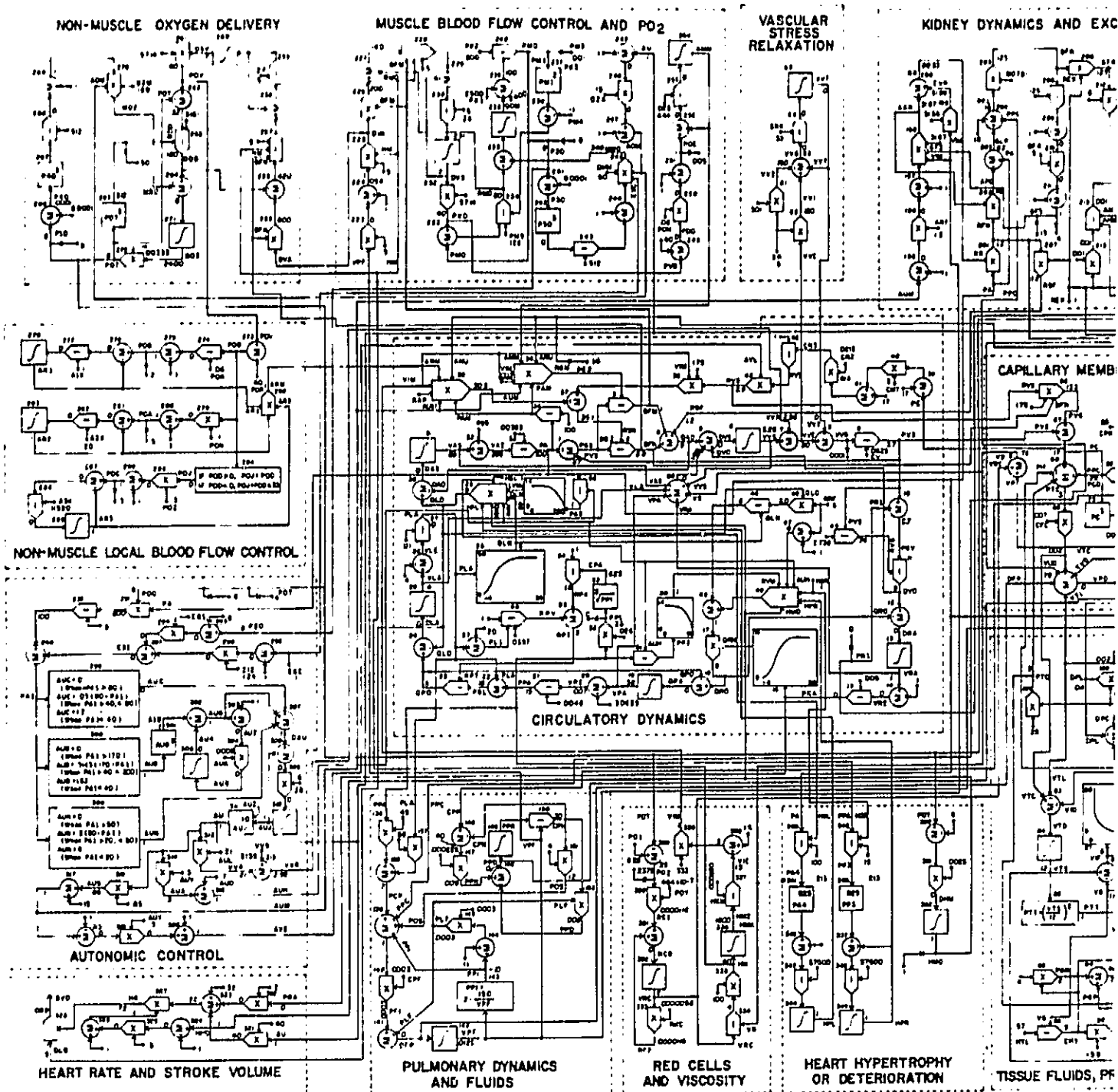
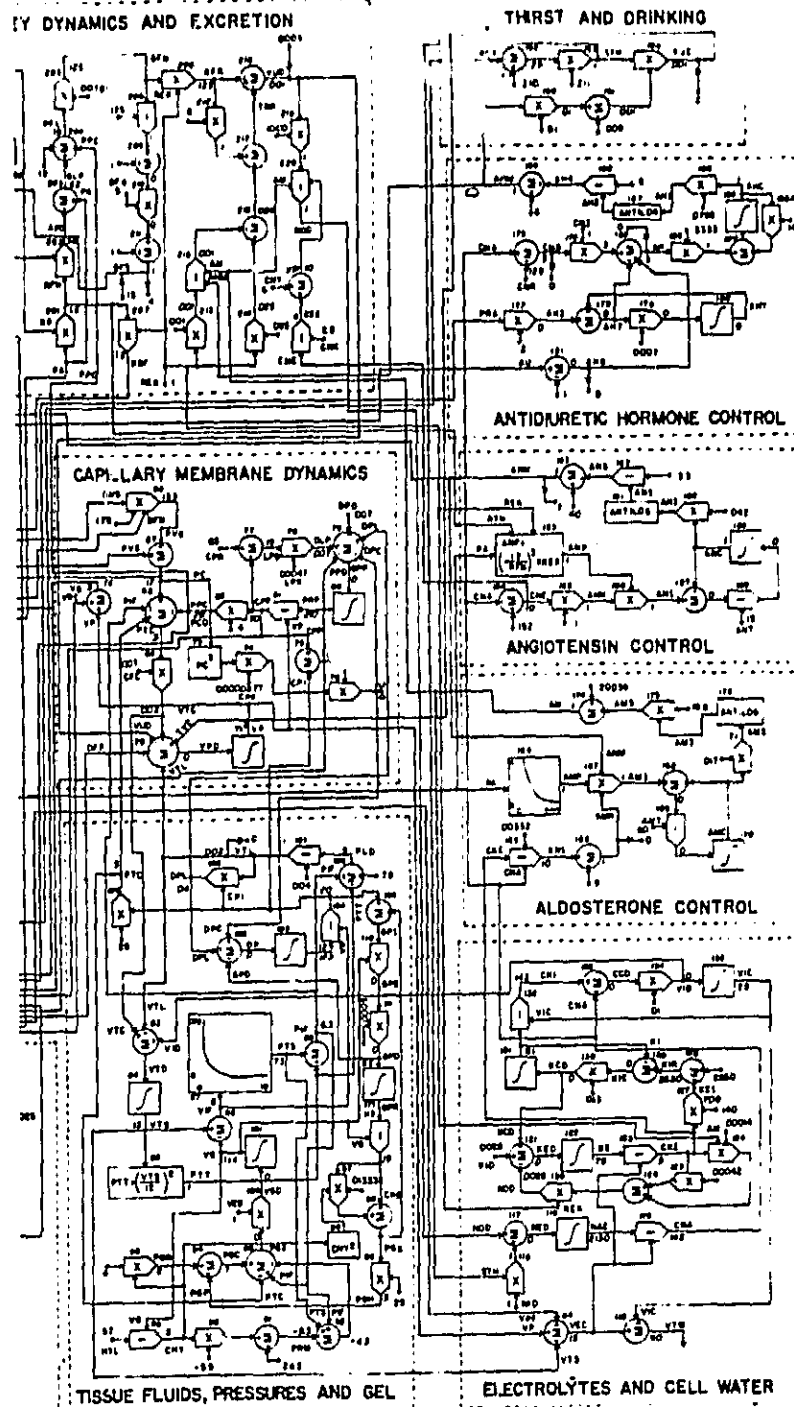


FIGURE C-1.—Systems analysis diagram for regulation of the circulation according to Guyton et al. Reprinted from reference C-1 with permission of the publisher. Units are the following: volume in liters; mass in grams; time in minutes; chemical units in milli-equivalents; pressure in millimeters of mercury; and control factors in arbitrary units but in most instances expressed as the ratio to normal—for instance, a value of 1 represents normal. Normal values are given on the lines that represent the respective variables. The important dependent and independent variables in the analysis are listed in the key. Additional variables are present for purposes of calculation but generally have no physiological significance.

ORIGINAL PAGE IS
OF POOR QUALITY

KEY



- AAR*—afferent arteriolar resistance
- AHM*—antidiuretic hormone multiplier, ratio of normal effect
- AM*—aldosterone multiplier, ratio of normal effect
- AMC*—aldosterone concentration
- AMM*—muscle vascular constriction caused by local tissue control, ratio to resting state
- AMP*—effect of arterial pressure on rate of aldosterone secretion
- AMR*—effect of sodium to potassium ratio on aldosterone secretion rate
- AMT*—time constant of aldosterone accumulation and destruction
- ANC*—angiotensin concentration
- ANM*—angiotensin multiplier effect on vascular resistance, ratio to normal
- ANN*—effect of sodium concentration on rate of angiotensin formation
- ANP*—effect of renal blood flow on angiotensin formation
- ANT*—time constant of angiotensin accumulation and destruction
- ANU*—nonrenal effect of angiotensin
- AOM*—autonomic effect on tissue oxygen utilization
- APD*—afferent arteriolar pressure drop
- ARF*—intensity of sympathetic effects on renal function
- ARM*—vasoconstrictor effect of all types of autoregulation
- AR1*—vasoconstrictor effect of rapid autoregulation
- AR2*—vasoconstrictor effects of intermediate autoregulation
- AR3*—vasoconstrictor effect of long-term autoregulation
- AU*—overall activity of autonomic system, ratio to normal
- AUB*—effect of baroreceptors on autoregulation
- AUC*—effect of chemoreceptors on autonomic stimulation
- AUH*—autonomic stimulation of heart, ratio to normal
- AUK*—time constant of baroreceptor adaptation
- AUL*—sensitivity of sympathetic control of vascular capacitance
- AUM*—sympathetic vasoconstrictor effect on arteries
- AUN*—effect of CNS ischemic reflex on autoregulation
- AUV*—sensitivity control of autonomic control on heart function
- AUY*—sensitivity of sympathetic control of veins
- AUZ*—overall sensitivity of autonomic control
- AVE*—sympathetic vasoconstrictor effect on veins
- AIK*—time constant of rapid autoregulation
- A2K*—time constant of intermediate autoregulation
- A3K*—time constant of long-term autoregulation
- A4K*—time constant for muscle local vascular response to metabolic activity
- BFM*—muscle blood flow
- BFN*—blood flow in nonmuscle, nonrenal tissues
- CA*—capacitance of systemic arteries
- CCD*—concentration gradient across cell membrane
- CHY*—concentration of hyaluronic acid in tissue fluids
- CKE*—extracellular potassium concentration

FIGURE C-1.—Continued.

<i>CKI</i> —intracellular potassium concentration	<i>O₂M</i> —basic oxygen utilization in nonmuscle body tissues
<i>CNA</i> —extracellular sodium concentration	<i>PA</i> —aortic pressure
<i>CNE</i> —sodium concentration abnormality causing third factor effect	<i>PAM</i> —effect of arterial pressure in distending arteries, ratio to normal
<i>CPG</i> —concentration of protein in tissue gel	<i>PC</i> —capillary pressure
<i>CPI</i> —concentration of protein in free interstitial fluid	<i>PCD</i> —net pressure gradient across capillary membrane
<i>CPN</i> —concentration of protein in pulmonary fluids	<i>PCP</i> —pulmonary capillary pressure
<i>CPP</i> —plasma protein concentration	<i>PDO</i> —difference between muscle venous oxygen pO_2 and normal venous oxygen pO_2
<i>CV</i> —venous capacitance	<i>PFI</i> —rate of transfer of fluid across pulmonary capillaries
<i>DAS</i> —rate of volume increase of systemic arteries	<i>PFL</i> —renal filtration pressure
<i>DFF</i> —rate of increase in pulmonary free fluid	<i>PGC</i> —colloid osmotic pressure of tissue gel
<i>DHM</i> —rate of cardiac deterioration caused by hypoxia	<i>PGH</i> —absorbency effect of gel caused by recoil of gel reticulum
<i>DLA</i> —rate of volume increase in pulmonary veins and left atrium	<i>PGL</i> —pressure gradient in lungs
<i>DLP</i> —rate of formation of plasma protein by liver	<i>PGP</i> —colloid osmotic pressure of tissue gel caused by entrapped protein
<i>DOB</i> —rate of oxygen delivery to nonmuscle cells	<i>PGR</i> —colloid osmotic pressure of interstitial gel caused by Donnan equilibrium
<i>DPA</i> —rate of increase in pulmonary volume	<i>PGV</i> —pressure from veins to right atrium
<i>DPC</i> —rate of loss of plasma proteins through systemic capillaries	<i>PIF</i> —interstitial fluid pressure
<i>DPI</i> —rate of change of protein in free interstitial fluid	<i>PLA</i> —left atrial pressure
<i>DPL</i> —rate of systemic lymphatic return of protein	<i>PLD</i> —pressure gradient to cause lymphatic flow
<i>DPO</i> —rate of loss of plasma protein	<i>PLF</i> —pulmonary lymphatic flow
<i>DRA</i> —rate of increase in right atrial volume	<i>PMO</i> —muscle cell pO_2
<i>DVS</i> —rate of increase in venous vascular volume	<i>POD</i> —nonmuscle venous pO_2 minus normal value
<i>EVR</i> —postglomerular resistance	<i>POK</i> —sensitivity of rapid system of autoregulation
<i>EXC</i> —exercise activity, ratio to activity at rest	<i>PON</i> —sensitivity of intermediate autoregulation
<i>EXE</i> —exercise effect on autonomic stimulation	<i>POS</i> —pulmonary interstitial fluid colloid osmotic pressure
<i>GFN</i> —glomerular filtration rate of undamaged kidney	<i>POT</i> —nonmuscle cell pO_2
<i>GFR</i> —glomerular filtration rate	<i>POV</i> —nonmuscle venous pO_2
<i>GLP</i> —glomerular pressure	<i>POY</i> —sensitivity of red cell production
<i>GPD</i> —rate of increase of protein in gel	<i>POZ</i> —sensitivity of long-term autoregulation
<i>GPR</i> —total protein in gel	<i>PO₂</i> —oxygen deficit factor causing red cell production
<i>HM</i> —hematocrit	<i>PPA</i> —pulmonary arterial pressure
<i>HMD</i> —cardiac depressant effect of hypoxia	<i>PPC</i> —plasma colloid osmotic pressure
<i>HPL</i> —hypertrophy effect on left ventricle	<i>PPD</i> —rate of change of protein in pulmonary fluids
<i>HPR</i> —hypertrophy effect on heart, ratio to normal	<i>PPI</i> —pulmonary interstitial fluid pressure
<i>HR</i> —heart rate	<i>PPN</i> —rate of pulmonary capillary protein loss
<i>HSL</i> —basic left ventricular strength	<i>PPO</i> —pulmonary lymph protein flow
<i>HSR</i> —basic strength of right ventricle	<i>PPR</i> —total protein in pulmonary fluids
<i>HYL</i> —quantity of hyaluronic acid in tissues	<i>PRA</i> —right atrial pressure
<i>IFP</i> —interstitial fluid protein	<i>PRM</i> —pressure caused by compression of interstitial fluid gel reticulum
<i>KCD</i> —rate of change of potassium concentration	<i>PRP</i> —total plasma protein
<i>KE</i> —total extracellular fluid potassium	<i>PTC</i> —interstitial fluid colloid osmotic pressure
<i>KED</i> —rate of change of extracellular fluid concentration	<i>PTS</i> —solid tissue pressure
<i>KI</i> —total intracellular potassium concentration	<i>PTT</i> —total tissue pressure
<i>KID</i> —rate of potassium intake	<i>PVG</i> —venous pressure gradient
<i>KOD</i> —rate of renal loss of potassium	<i>PVO</i> —muscle venous pO_2
<i>LVM</i> —effect of aortic pressure on left ventricular output	<i>PVS</i> —average venous pressure
<i>MMO</i> —rate of oxygen utilization by muscle cells	<i>QAO</i> —blood flow in the systemic arterial system
<i>MO₂</i> —rate of oxygen utilization by nonmuscle cells	<i>QLN</i> —basic left ventricular output
<i>NAE</i> —total extracellular sodium	<i>QLO</i> —output of left ventricle
<i>NED</i> —rate of change of sodium in intracellular fluids	<i>QOM</i> —total volume of oxygen in muscle cells
<i>NID</i> —rate of sodium intake	<i>QO₂</i> —nonmuscle total cellular oxygen
<i>NOD</i> —rate of renal excretion of sodium	<i>QPO</i> —rate of blood flow into pulmonary veins and left atrium
<i>OMM</i> —muscle oxygen utilization at rest	<i>QRF</i> —feedback effect of left ventricular function on right ventricular function
<i>OSA</i> —aortic oxygen saturation	<i>QRN</i> —basic right ventricular output
<i>OSV</i> —nonmuscle venous oxygen saturation	
<i>OVA</i> —oxygen volume in aortic blood	
<i>OVS</i> —muscle venous oxygen saturation	

FIGURE C-1.—Continued.

QRO—actual right ventricular output
QVO—rate of blood flow from veins into right atrium
RAM—basic vascular resistance of muscles
RAR—basic resistance of nonmuscular and nonrenal arteries
RBF—renal blood flow
RCI—red cell production rate
RC2—red cell destruction rate
RCD—rate of change of red cell mass
REN—percent of normal renal function
RFN—renal blood flow if kidney is not damaged
RKC—rate factor for red cell destruction
RMO—rate of oxygen transport to muscle cells
RPA—pulmonary arterial resistance
RPT—pulmonary vascular resistance
RPV—pulmonary venous resistance
RR—renal resistance
RSM—vascular resistance in muscles
RSN—vascular resistance in nonmuscle, nonrenal tissues
RVG—resistance from veins to right atrium
RVM—depressing effect on right ventricle of pulmonary arterial pressure
RVS—venous resistance
SR—intensity factor for stress relaxation
SRK—time constant for stress relaxation
STH—effect of tissue hypoxia on salt and water intake
SVQ—stroke volume output
TRR—tubular reabsorption rate
TVD—rate of drinking
VAS—volume in systemic arteries

VB—blood volume
VEC—extracellular fluid volume
VG—volume of interstitial fluid gel
VGD—rate of change of tissue gel volumes
VIB—blood viscosity, ratio to that of water
VIC—cell volume
VID—rate of fluid transfer between interstitial fluid and cells
VIE—portion of blood viscosity caused by red blood cells
VIF—volume of free interstitial fluid
VIM—blood viscosity, ratio to normal blood
VLA—volume in left atrium
VP—plasma volume
VPA—volume in pulmonary arteries
VPD—rate of change of plasma volume
VPF—pulmonary free fluid volume
VRA—right atrial volume
VRC—volume of red blood cells
VTC—rate of fluid transfer across systemic capillary membranes
VTD—rate of volume change in total interstitial fluid
VTL—rate of systemic lymph flow
VTS—total interstitial fluid volume
VTW—total body water
VUD—rate of urinary output
VV7—increased vascular volume caused by stress relaxation
VVR—diminished vascular volume caused by sympathetic stimulation
VVS—venous vascular volume
Z8—time constant of autonomic response

FIGURE C-1.—Concluded.

tissue are similar to that of the nonmuscle, non-renal precapillary and postcapillary resistances in the original Guyton model with the following exceptions.

First, the passive distention effect resulting from hydrostatic pressure was not included as a determinant of the leg arteriolar resistance. This exclusion was based on the belief that, upon standing, a strong myogenic local reflex acts to constrict arteriolar vessels (as well as capillary sphincters) in response to the high hydrostatic load. The myogenic reflex opposes the passive distention effect. It was felt that the passive distention effect should be removed until the myogenic effect is included in the model. Otherwise, the effect of standing would create arteriolar distention great enough to overcome autonomic vasoconstriction, a condition that does not normally exist in the real physiological system.

Second, the veins are not known to participate in the myogenic response but, rather, should be highly responsive to passive distention under the high hydrostatic pressures of standing. Consequently, a

passive distention effect was added to the leg venule resistance. This formulation permitted a 0.13-kN/m^2 (1 mmHg) change in pressure to cause a 1-percent change in resistance in accordance with data reviewed by McDonald (ref. C-7). The net effect of excluding the passive distention effect in the leg arterioles and adding this effect to the leg venules is to favor a higher precapillary/postcapillary resistance ratio upon standing which tended to reduce leg capillary pressure towards leg venous pressure. According to Mellander (ref. C-8), this is an appropriate response to limit outward filtration of plasma in the erect posture.

EFFECT OF GRAVITY ON PRESSURE GRADIENTS

The average hydrostatic pressure gradient in the legs (PG_L) due to gravity has been expressed as

$$PG_L = H_L \times F \times \sin \phi \quad (C1)$$

TABLE C-1.—Steady-State Values of Major
Physiological Parameters in Modified Guyton Model

Parameter	Value	Parameter	Value
Blood volume, liters		Blood flow, liters/min	
Right heart	0.109	Cardiac output	6.47
Pulmonary	0.413	Renal	1.20
Left heart	0.431	Leg (muscle)	0.98
Total cardiopulmonary	0.953	Nonrenal, nonmuscle	4.30
Upper artery	0.714		
Leg artery	0.146	Body fluid volume, liters	
Total artery	0.860	Blood	5.003
Upper veins	2.750	Plasma	3.007
Leg veins	0.440	Red cell	1.999
Total veins	3.190	Interstitial	12.013
Total stressed volume	0.877	Free fluid	0.545
Total unstressed volume	4.126	Gel	11.467
Total upper body volume	4.417	Total body water	40.038
Total leg volume	0.586	Extracellular	15.042
Total blood volume	5.003	Intracellular	24.996
Blood pressure, kN/m ²		Metabolic rate, ml O ₂ /min	
Upper arterial	13.35	Nonmuscle, nonrenal	252
Leg arterial	13.24	Leg (muscle)	58
Upper venous	0.61	Total	310
Leg venous	0.65		
Right heart	0.08	Concentration, meq/liter	
Pulmonary	2.52	Plasma sodium	142.0
Left heart	0.129	Plasma potassium	5.00
		Plasma protein	70.1
Blood pressure, mmHg		Hematocrit, vol.%	39.95
Upper arterial	100.1		
Leg arterial	99.3	Stroke volume, liters	0.088
Upper venous	4.55		
Leg venous	4.89	Heart rate, beats/min	73.3
Right heart	0.63		
Pulmonary	18.87		
Left heart	0.970		

where H_L is taken as the distance (in centimeters) from the heart to the knees. (The knee was used as a convenient reference point to find the average hydrostatic effect in a lumped leg compartment.) The term F converts pressures from centimeters water to millimeters mercury, whereas ϕ is the angle (in radians) of body tilt measured from the horizontal. The pressure gradient PG_L is introduced into the formulation for leg flow at the input to the leg arterial compartment, where it aids flow, and at the output of the leg venous compartment, where it opposes flow.

The gravity effect on the carotid baroreceptors must also be included since the tilt angle changes the hydrostatic pressure at these important sensors. The hydrostatic gradient at the baroreceptors is

given by an equation similar to equation (C1) except that the term H_L is taken to be the distance between the heart and the carotid receptor. The pressure gradient so calculated is subtracted from the effective blood pressure sensed at the carotid body during a tilt simulation. Any angle of tilt may be simulated by adjusting ϕ , and other postures such as sitting may be studied by reducing the height H_L .

VENOUS VALVES

The effect of venous valves has been added by permitting blood flow from the venous leg compartment to assume only positive values. Because

this leg compartment can only be filled by arterial blood (rather than reverse venous flow from upper body veins), transient conditions can exist in which outflow to the veins is extremely low. This occurs, for example, during the onset of lower body negative pressure simulation. This situation was not possible in the original Guyton formulation.

LEG PLASMA/INTERSTITIAL FILTRATION

A mechanism was added to permit plasma to filter into a new interstitial leg compartment. This mechanism is illustrated in figure C-2 in schematic form. Blood flow in the leg tissues is driven under an arterial-venous pressure gradient ($PAL - PVL$) across an arterial resistance RAL and a venous resistance RVL . The capillary pressure ($PCLG$) is computed as a function of upstream and downstream pressures and the precapillary/postcapillary resistance ratio, in accordance with the Landis-Pappenheimer formulation:

$$PCLG = RCLG \cdot PAL + (1 - RCLG) \cdot PVL$$

where $RCLG = RVL / (RVL + RAL)$. Filtration rate into the leg interstitium ($QLEG$) is based on the transcapillary hydrostatic pressure and oncotic pressure gradients multiplied by a leg capillary filtration coefficient ($CFLG$).

$$QLEG = (PCLG - PILG - PPC) \cdot CFLG$$

where $PILG$ is the leg interstitial pressure and PPC is the plasma colloid osmotic pressure. It is assumed that interstitial colloid osmotic pressure is negligible. The value of $PILG$ is determined from the leg interstitial volume ($VILG$) and the tissue compliance ($CTLG$).

Because of the lack of detailed information regarding the leg tissues and tissue pressure changes during standing, this represents a highly simplified model of leg filtration having the following major assumptions.

1. Leg tissue fluid volume is equal to 1.5 liters in supine steady state.
2. Linear compliance permits tissue pressures to rise by about 5.3 kN/m² (40 mmHg) during standing when the fluid volume is increased by approximately 500 milliliters because of plasma filtration. This large pressure increase is necessary to oppose excessive filtration because of the equally high

change in capillary pressure.

3. The effects of lymph flow, tissue colloidal concentration, and tissue gel have not been included.

The total resistance to blood flow through the leg muscle is given by the sum of the two variable resistances

$$RL = RAL + RVL$$

and the blood flow rate of the leg is taken to be the difference of pressure between the leg arteries (PAL) and veins (PVL) divided by the resistance

$$QL = (PAL - PVL) / RL$$

EXTERNAL LEG VASCULAR PRESSURE

An external pressure term (PXV), shown in figure C-2, was included in the formulation for leg arterial and venous pressure, as was an external tissue pressure term (PXT). These terms are normally zero. By setting PXV and/or PXT to values less than zero, the effects of lower body negative pressure can be simulated. Values higher than zero will simulate various events such as positive pressure leg garments, water immersion, dehydration of the legs, and a muscle pump mechanism, all of which have the effect of reducing venous leg blood volume and aiding in venous return during standing.

INSTANTANEOUS STRESS RELAXATION EFFECT

A term representing instantaneous stress relaxation was added to the stress relaxation block of the original model. This term appears as a constant factor (normally zero), which was found to be necessary to aid venous return during tilt simulation. In that case, reverse stress relaxation was used. Its physiological counterpart may be a combination of stress relaxation and the abdominal compression postural reflex, as well as a central venoconstrictor effect.

MODIFIED RED BLOOD CELL PRODUCTION ALGORITHM

A new algorithm for red cell regulation was also implemented in the recompartimentalized Guyton model. This new block was based on the

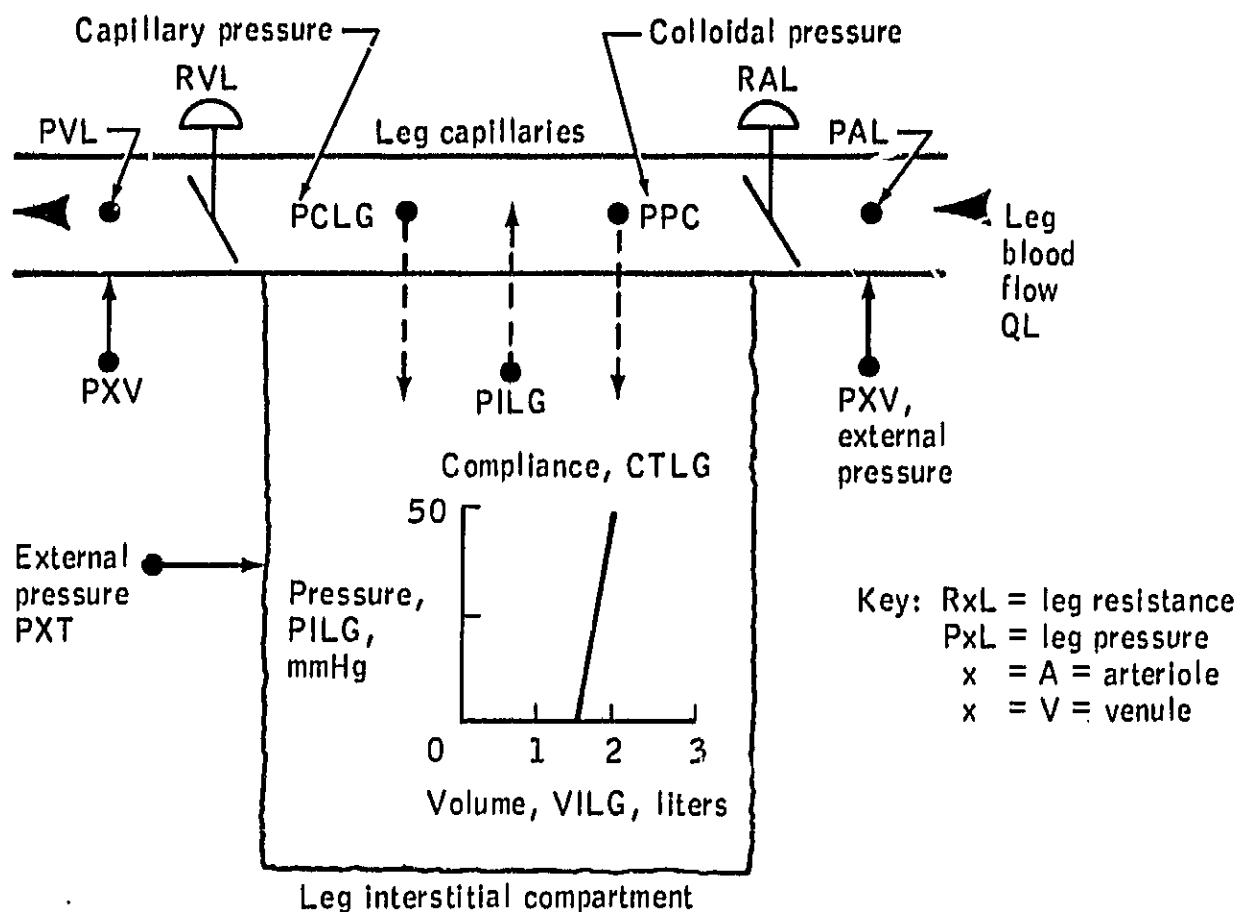


FIGURE C-2.—Schematic diagram of leg filtration mechanisms.

erythropoiesis regulatory simulation model previously described in Section III. This model has greater capability than the blood cell subroutine in the original Guyton model, especially with respect to the simulation of hemopoietic responses to hypoxia, red cell infusion, and bed rest. A detailed description of this algorithm, as it appears in the modified Guyton model, is presented in reference C-3.

The new red blood cell algorithm was based on a kidney sensor of oxygen partial pressure located in tissue of constant metabolic rate and perfused with venous capillary blood, flowing at a constant rate. These restrictions permit erythropoiesis to be responsive primarily to changes in hematocrit and arterial oxygen partial pressure, shifts of oxy-hemoglobin dissociation, and disturbances in oxygen-carrying capacity of hemoglobin.

RENIN-ANGIOTENSIN SYSTEM

The original version of the Guyton model did not possess a detailed representation of the renin-angiotensin system. In particular, renin secretion as such was not present, and the model did not respond correctly to low-level angiotensin II infusion. This original model contained what was essentially a black box, with angiotensin level dependent on tubular sodium flow. To extend the range of applicability of the model, the black box was replaced with a more physiologically oriented section. A flow chart of the added system is contained in appendix A (fig. A-3). The new system improved the mechanism for releasing angiotensin into the circulation and permitted thirst and salt intake as well as renal afferent and efferent arteriolar resistances to depend on angiotensin levels.

BARORECEPTOR SYSTEM

The baroreceptor system in the original Guyton model was changed by direct inclusion of separate aortic and carotid effects and by separate inclusion of the autonomic influence on both contractility of the heart and whole-body unstressed volume. Appropriate delays and resetting mechanisms were used. A flow chart for the modified system is given in figure C-3.

VASCULAR STRESS RELAXATION

Stress relaxation of the vascular system was extended by the inclusion of new components with different time constants for action. These new components are associated with 6-hour and 14-day relaxation phenomena.

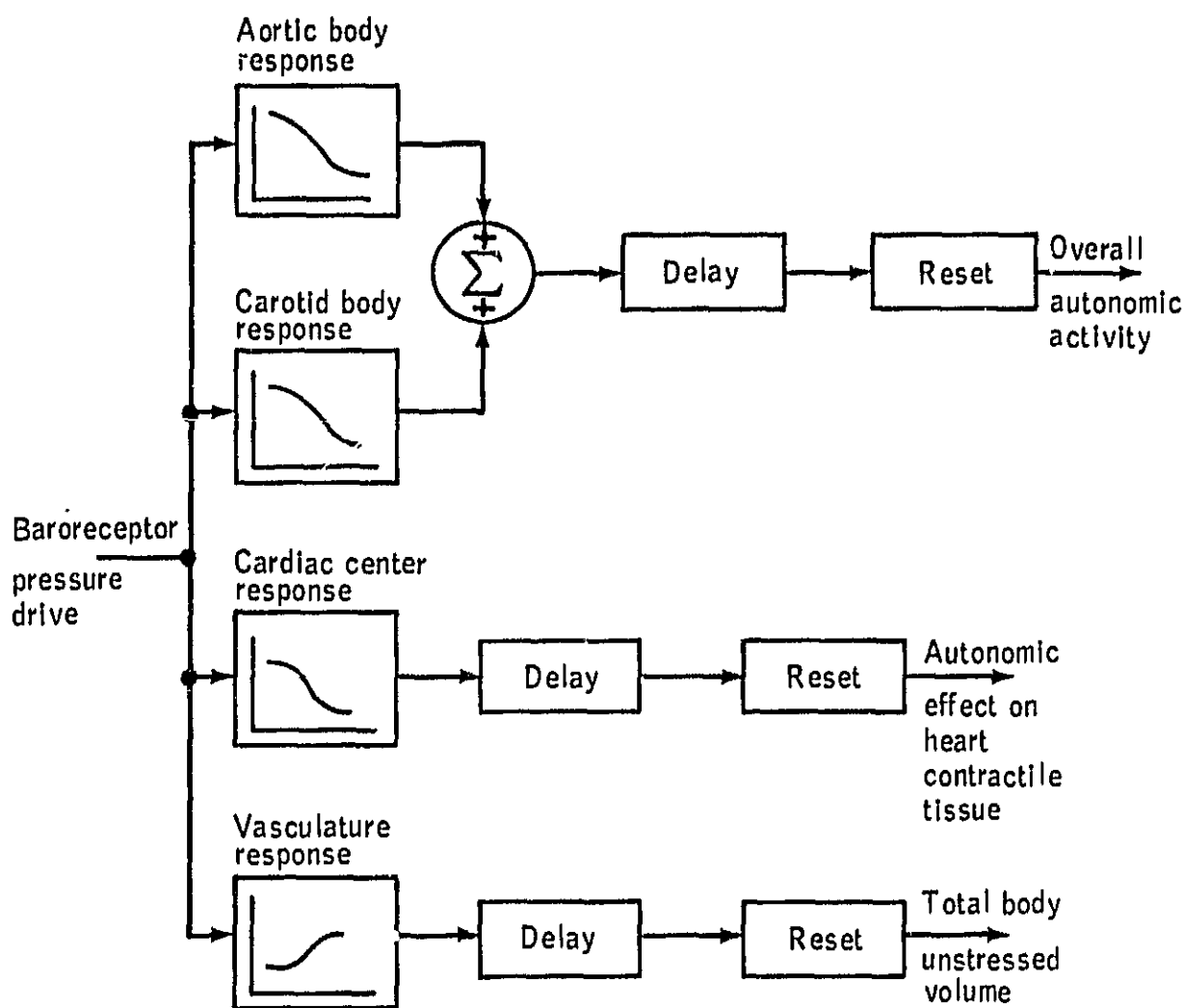


FIGURE C-3.—Block diagram of baroreceptor system.

REFERENCES

- C-1. Guyton, A. C.; Coleman, T. G.; and Granger, H. J.: Circulation: Overall Regulation. *Ann. Rev. Physiol.*, vol. 34, 1972, pp. 13-46.
- C-2. Guyton, A. C.; Jones, Carl; and Coleman, T. G.: *Circulatory Physiology: Cardiac Output and Its Regulation*. Second ed. W. B. Saunders Co. (Philadelphia), 1973.
- C-3. Leonard, J. I.; and Grounds, D. J.: Study Report: Modification of the Long Term Circulatory Model for the Simulation of Bed Rest. (General Electric Co., Houston, Tex.; TIR 742-LSP-7011.) NASA CR-160186, 1977.
- C-4. White, R. J.: A Long Term Model of Circulation: Final Report. (General Electric Co., Houston, Tex.; TIR 741-MED-4021.) NASA CR-147674, 1974.
- C-5. White, R. J.: Summary Report on a Basic Model of Circulatory, Fluid, and Electrolyte Regulation in the Human System Based Upon the Model of Guyton. (General Electric Co., Houston, Tex.; TIR 741-MED-3042.) NASA CR-160212, 1973.
- C-6. Archer, G. T.: User's Instructions for the Guyton Circulatory Dynamics Model Using the Univac 1110 Batch and Demand Processing (With Graphics Capabilities) Rep. TIR 741-MED-4004, General Electric Co. (Houston, Tex.), 1974.
- C-7. McDonald, Donald Arthur: *Blood Flow in Arteries*. Williams and Wilkins Co. (Baltimore), 1960.
- C-8. Mellander, S.: Interaction of Local and Nervous Factors in Vascular Control. *Angiologica*, vol. 8, 1971, pp. 187-201.